

# Distribution of Spectral Characteristics and the Cosmological Evolution of GRBs.

Nicole M. Lloyd and Vahé Petrosian

Center for Space Sciences and Astrophysics, Stanford University

## ABSTRACT

We investigate the cosmological evolution of GRBs, using the total gamma ray fluence as a measure of the burst strength. This involves an understanding of the distributions of the spectral parameters of GRBs as well as the total fluence distribution - both of which are subject to detector selection effects. We present new non-parametric statistical techniques to account for these effects, and use these methods to estimate the true distribution of the peak of the  $\nu F_\nu$  spectrum,  $E_p$  from the raw distribution. The distributions are obtained from four channel data and therefore are rough estimates. Here, we emphasize the methods and present qualitative results. Given its spectral parameters, we then calculate the total fluence for each burst, and compute its cumulative and differential distributions. We use these distributions to estimate the cosmological rate evolution of GRBs, for three cosmological models. Our two main conclusions are the following: 1) Given our estimates of the spectral parameters, we find that there may exist a significant population of high  $E_p$  bursts that are not detected by BATSE, 2) We find a GRB co-moving rate density quite different from that of other extragalactic objects; in particular, it is different from the recently determined star formation rate.

*Subject headings:* gamma rays: bursts – methods: statistical – cosmology: observations – miscellaneous.

## 1. Introduction

Identification of several gamma-ray bursts (hereafter GRBs) with X-ray, optical and radio afterglows, as well as measurements of the redshifts of GRB 970508 and GRB 981214 are beginning to define the GRB paradigm. However, this information is not sufficient for detailed cosmological studies of their distribution and evolution. Until more information on the distances to GRBs are revealed, we must continue to rely on standard statistical studies (such as obtaining number count distributions of fluence or flux) to gain further insight on the nature of these events.

However, information on the spatial distribution - although necessary - will not be sufficient for solving the puzzle of GRBs. In particular, we need spectral information to understand the energy release and radiation processes at the burst. This paper deals with the determination of

the spatial and spectral properties of GRBs. As we discuss below, these two distributions are related, and we need to determine them simultaneously.

The information on the spatial distribution comes primarily from the investigation of source counts or the  $\log N$ - $\log S$  relation. Assuming a luminosity function (LF) and a cosmological model, one can convert such counts to spatial (or redshift) distributions (Weinberg, 1972). The likelihood of the assumed luminosity function determines our confidence in the redshift distribution or cosmological evolution of these sources. The usual practice is to use the peak flux  $f_p(\nu)$  as a measure of the burst strength. This flux is related to the peak luminosity  $L_p(\nu)$  via  $L_p(\nu) = f_p(\nu)4\pi d_L^2 K(z)$ , where  $d_L(z)$  is the luminosity distance, and  $K(z)$  is the so-called K-correction due to redshift of the spectrum. However, we have no knowledge of the burst peak luminosity function - say  $\Psi(L_p(\nu))$  - and it is unclear what assumptions can be made about this function. For example, in a fireball model, both the duration and the peak luminosities are expected to depend on the details of the fireball (e.g. the bulk Lorentz factor and amount of baryon loading), so that their distributions will be broad and perhaps comparable to the observed range of the peak fluxes. As a result, the luminosity function cannot be readily de-convolved from the spatial distribution, and we cannot get an accurate measure of the burst evolution or spatial distribution from the  $\log N$ - $\log S$  diagram.

On the other hand, in a neutron star (or black hole) merger model, the total energy released ( $E_{tot}$ )- represented by the gravitational potential energy of the merging process - is expected to be well defined and have a narrow distribution; this is also most likely true for the “hypernova” model. It is therefore more plausible that the total radiated energy (integrated over time) may also have a narrow distribution. The question that remains is what radiative signature is a representative measure of this energy and the strength of the GRB.

As the name “gamma ray burst” implies, the peak gamma-ray flux  $f_p$  (or luminosity  $L_p$ ) of a GRB far exceeds the peak fluxes at other energies. However, until recently, we did not know at what frequency the total radiated energy peaked. The recent X-ray, optical and radio observations of the afterglows - in particular the fact that these fluxes decline more rapidly than  $1/t$  (see e.g. Murakami et al., 1997, Galama et al., 1997) - indicate that the energy **fluence**  $F$ , and therefore the total radiated energy  $E_o$ , in the gamma-ray range is also higher than in any other band. The radiated energy  $E_o$  is less than, but proportional to, the total released energy  $E_{tot}$ . Then the radiated energy distribution  $\Psi(E_o)$  may have a narrow distribution. Thus, the gamma-ray fluence  $F$  may provide the best measure of the strength of the burst for the  $\log N$ - $\log S$  analysis and other investigations.

However, even the observed fluence may not be ideal for the task at hand, because this usually represents the fluence in some narrow energy range (i.e. the energy range in which the detector triggers). A better measure will be a bolometric fluence  $F_{tot} = \int F(\nu)d\nu$ , where the integral extends over the gamma-ray range of photon frequencies  $\nu$ . This is because  $F_{tot}$  is related to the total radiated energy as  $E_o = 4\pi d_L^2 F_{tot}(1+z)$ , where we have assumed that the burst

radiates isotropically. Note that the relation between the monochromatic flux (or fluence) and the corresponding luminosities require a knowledge of the so called K-correction due to redshift of the spectrum. This complication is not present in the above relation between the total energy and the “bolometric” fluence. It is also important to note that  $F_{tot}$  depends on the spectral properties of the burst. Hence, if we want to simplify matters by dealing with the total fluence, we need to understand the spectral distribution  $F(\nu)$  of the GRBs.

The primary goal of this paper is to demonstrate how we can obtain information on the cosmological evolution of GRBs, using the observed distribution of  $F_{tot}$ . However, for an accurate bias free determination of the distribution of  $F_{tot}$ , we need to determine the spectral parameters of each burst. It is common to use the following four parameters (say, in a Band spectrum (1993)) to characterize a burst’s spectrum: the photon energy at the peak of the  $\nu F_\nu$  spectrum,  $E_p$ , the low energy spectral index,  $\alpha$ , the high energy spectral index  $\beta$ , and a normalization  $A$ . The best source of data for the purpose of determining these parameters and  $F_{tot}$  is the BATSE instrument on board the Compton Gamma-Ray Observatory (CGRO). However, because the BATSE trigger criterion is based on photon counts between 50 - 300 keV (for the 3B catalog), the selection biases or thresholds on  $F_{tot}$  as well as the spectral parameters can be quite complicated. In §2 we show how the trigger criterion used by BATSE can be used to obtain the selection bias on any measured quantity - in particular, the  $F_{tot}$  and  $E_p$  - and describe new methods to account for the resultant complicated data truncation. In §3, we present our results on the determination of the spectral parameters. The distribution of  $E_p$  is given in §4, and in §5 we derive the distribution of  $F_{tot}$ , give a scenario for cosmological evolutions of the GRBs, and discuss its relation to the new observations of afterglows and evolution of other cosmological sources. A brief summary is presented in §6.

## 2. Description of Data and The Basic Problem

### 2.1. The Data

BATSE has produced a large catalog of GRBs with a wealth of information on their temporal and spectral characteristics. This detector has been designed to optimally detect GRBs and has been very successful in achieving this goal. Nevertheless, like all detectors, it has intrinsic limitations and may miss certain types of bursts or provide only limited information on others. BATSE is a triggered instrument; it will record data on a burst if the detector counts in a time interval  $\Delta t$  and energy range  $\Delta E$  exceed some threshold value  $C_{min}(\Delta t)$  determined by the background fluctuations. BATSE uses three trigger time intervals  $\Delta t = 1024, 256,$  and  $64$  ms with four energy channels  $\Delta E = 25 - 50, 50 - 100, 100 - 300,$  and  $> 300$  keV. For most of the data, triggering is based on counts in channels 2 and 3; recently, however, other channel combinations have been tried. Here we will use the 4 channel LAD fluence values published in the BATSE 3B catalog (Meegan et al., 1995), which utilizes the former trigger scheme. However, the formalism described below is applicable to the latter data as well. Note that we analyze bursts with

$C_{max}/C_{min}$  on 1024ms timescale. Because of the lack of resolution of the four channel data, here we will emphasize the method of our calculations rather than give concrete quantitative results. Future work will involve calculations made from 16 channel CONT data.

## 2.2. Data Truncation

The BATSE detector trigger conditions lead to several limitations on the data. The most obvious is that only bursts with peak counts  $C_{max} > C_{min}$  are detected. Determination of the average  $V/V_{max} = (C_{min}/C_{max})^{3/2}$ , and its distribution were one of the primary objectives of BATSE using this trigger configuration (Meegan et al., 1992). Another limitation arises from the finite durations  $\Delta t$  of the triggering criteria. As pointed out by Petrosian and Lee (1994, see also Lee and Petrosian, 1996), this reduces the detector efficiency of short duration bursts (duration  $T < \Delta t$ ) in the sense that there is a relative bias against detection of weaker bursts with shorter duration. Similarly, as pointed out by Piran and Narayan (1996), the finite range  $\Delta E$  of the detector energy channels provides another limitation. In this case, the detector efficiency is highest for bursts with most of their photons in the range  $\Delta E$ , and decreases for bursts with more of their flux outside this range.

It turns out that we can account for these limitations by utilizing the BATSE trigger condition: Let us consider a burst characteristic, say  $X$ , whose value is measured by BATSE. For each burst, then, we know  $X$ ,  $C_{max}$ , and  $C_{min}$ . Now, in the spirit of the  $V/V_{max}$  test, one can ask what is the possible range of values of  $X$  that this burst can have and still trigger the instrument. In general,  $X$  can have an upper limit  $u$ , a lower limit  $l$ , or both limits;  $X \in T = [l, u]$ . This question was first posed by Petrosian and Lee (1996) in connection with the determination of the detection threshold or efficiency of the observed energy fluence  $F$ ; in this case, the fluence has only a lower limit  $F_{lim}$ . It was shown that this threshold (or for that matter, the threshold on any other measure of burst strength which is proportional to the photon counts) is obtained from the simple relation

$$F/F_{lim} = C_{max}/C_{min}, \tag{1}$$

provided the burst's spectrum does not change drastically throughout its duration.

For other bursts characteristics, this may not be the case. For example, we have shown (Lloyd and Petrosian 1998) that the spectral parameter  $E_p$  has both an upper and lower limit. The values of  $E_{p,max}$  and  $E_{p,min}$  are not related to  $C_{max}/C_{min}$  and  $E_p$  in a simple form as above, and thus we require a more complex procedure to determine their values. We will describe this in §3. Given the thresholds, we can then use non-parametric statistical techniques to obtain an estimate the parent distribution of the relevant observable from the observed distribution.

## 2.3. Dealing with Data Truncation

Correcting for data truncation in the one-sided case was discussed in detail by Efron and Petrosian (1992). This method has been used to determine the correlation between parameters in a bivariate (or multivariate) setting, and to obtain univariate distributions of several GRB characteristics (see, e.g., Lee and Petrosian, 1996). The basic idea is that one can use information from the untruncated region of a distribution to estimate how much data is missed due to the truncation. For a description of the basic process, see also Petrosian (1992 or 1993).

Dealing with data which has both upper and lower limits is more complex and requires a generalization of the above technique. Recently, Efron and Petrosian (1998) have developed a method to deal with this kind of data truncation. We briefly review this method here.

Consider data points  $(x_i, y_i)$  (in our case  $(E_p, F_{obs})$ ), where  $x_i$  has lower and upper limits  $l_i$  and  $u_i$ , respectively;  $x_i \in T_i = [l_i, u_i]$ . Let us also assume that  $x_i$  and  $y_i$  are uncorrelated. Let  $f(x)$  be the true distribution of  $x$ , which would be observed if there were no truncations. However, because  $x_i$  is limited to  $T_i$ , we observe the conditional distribution  $f(x_i|T_i) = f(x_i)/F(T_i)$ , where  $F(T_i) = [\sum_j f(x_j) : x_j \in T_i]$  is the probability that  $x$  exists in  $T_i$ . We normalize  $f(x_i)$  such that  $\sum_{i=1}^N f_i = 1$ , and define the vectors

$$f_i = f(x_i) \quad \text{and} \quad F_i = F(T_i) \tag{2}$$

and the matrix

$$J_{ij} = \begin{cases} 1, & x_j \in T_i, \\ 0, & x_j \notin T_i. \end{cases} \tag{3}$$

Furthermore, by definition, one can show that  $F_i = J_{ij} f_j$  (where we have used the convention that repeated indices are summed over). The goal is to estimate  $f(x)$  from  $l_i, u_i$ , and  $x_i$  assuming all  $N$  cases are independently distributed. It can be shown that maximizing the likelihood (see Maloney et al., 1998) of the observed data set gives

$$1/f_i = J_{ji} * (1/F_j) + \text{const}, \tag{4}$$

where  $J_{ji}$  is the transpose of  $J_{ij}$ . The procedure amounts to solving this equation iteratively, under the normalization condition and definition of  $F_j$  and  $J_{ij}$  given above. Convergence is reached when *const* in the above equation goes to zero. This method can be used to determine univariate cumulative ( $F$ ) and differential ( $f$ ) distributions. As described in Efron and Petrosian (1998), it can also be used to determine correlations between relevant variables (e.g. fluence and  $E_p$  or peak flux and  $E_p$ ).

We will use the methods described above to correct for data truncations and produce bias free distributions of the peak energy  $E_p$  and the total fluence  $F_{tot}$ ; we will then directly use the latter distribution to investigate the cosmological evolution of GRBs.

### 3. Spectral Characteristics

The spectral properties of GRBs provide the most direct information about the physical processes associated with the event. In particular, the distribution of the spectral parameters and the correlation between these and other GRB characteristics can shed significant light on the radiation mechanisms and energy production of the burst.

Therefore, our first task is to determine the spectral parameters of each burst. We characterize the spectral forms of the bursts by four parameters -  $\alpha$  and  $\beta$  (the photon power law index at low and high energies respectively),  $E_o$  (a break energy related to the peak of the  $\nu F_\nu$  spectrum) and  $A$  (a normalization in units of *ergs/cm<sup>2</sup>*). We choose two functional forms to represent the **energy** fluence spectra - a Band spectrum, and a generic double power-law spectrum with a smooth transition between the low energy and high energy power law behavior:

$$F(E) = \begin{cases} (A/E_o)(E/E_o)^{\alpha+1}\exp[(\beta - \alpha)(E/E_o - 1)], & E < E_o \\ (A/E_o)(E/E_o)^{\beta+1}, & E > E_o \end{cases} \quad (5)$$

$$F(E) = \frac{(A/E_o)(E/E_o)^{\alpha+1}}{1 + (E/E_o)^{\alpha-\beta}} \quad (6)$$

We are interested in bursts whose  $\nu F_\nu$  spectra have a maximum, so that we may correctly speak of  $E_p$  as the “peak of  $\nu F_\nu$ ”. To define  $E_p$  (as well as to keep the burst’s total fluence  $F_{tot}$  finite), we require  $\alpha$  to be greater than -2 and  $\beta$  to be less than -2 (which also implies  $\alpha > \beta$ ). As we discuss below, this does not impose any large bias in our sample. Then, with these constraints, we can define  $E_p$  for each spectrum above:  $E_p = E_o(\frac{\alpha+2}{\alpha-\beta})$  and  $E_p = E_o(\frac{-(\beta+2)}{\alpha+2})^{\frac{1}{\beta-\alpha}}$  for (5) and (6), respectively.

From four channel data, we can determine the four spectral parameters with no degrees of freedom. However, this introduces strong interplay between  $E_p$  and  $\beta$  or  $\alpha$ . We avoid this by selecting  $\beta$  from an assumed gaussian distribution with a mean of  $\approx -3$ , and a standard deviation of 1 (and of course the constraint  $\beta < -2$ ). This allows for one degree of freedom. In fact, we have performed this analysis using several distributions for  $\beta$  (i.e. a uniform distribution, or a gaussian with a different mean and standard deviation), and have found similar qualitative results. However, we should note that steeper, more negative  $\beta$ ’s will naturally produce higher  $E_p$ ’s, to accomodate the fluence in high energy channels (3 and 4). We find the rest of the parameters by minimizing  $\chi^2$  via a downhill simplex routine (e.g. see Press et al., 1992). For the Band spectrum, we find acceptable fits for 291 bursts, while 268 give acceptable fits for the second spectrum listed above, out of a total of 518 bursts. Figures 1a and 1b show the raw distributions of the spectral parameters obtained with this method for the two spectral forms in equation 5 and 6, respectively.

It turns out that the distribution of the parameters for bursts with unacceptably high  $\chi^2$  is not very different from those with acceptable  $\chi^2$ . We have tested to see if the reason for many high  $\chi^2$  bursts came from the constraints on  $\alpha$  and  $\beta$  mentioned above. Relaxing these restrictions, we found that only  $\sim 1\%$  of bursts that gave acceptable fits had an  $\alpha < -2$ ,  $\beta > -2$ , or  $\alpha > \beta$ . We therefore assume that the bursts with good fits are representative of the total sample. However,

because the lack of energy resolution of the four channel data, we would like to emphasize that our fits are rough estimates of the actual spectral parameters, so that the following analysis exhibits our method rather than presenting a final quantitative result. As mentioned previously, in future work we will use fits from 16 channel CONT data, which will provide a more accurate determination of these parameters.

Several studies have obtained the spectral parameters for the brightest GRBs (e.g., Band et al. 1993) and investigated correlations between these parameters and peak flux, duration and spatial distributions (Malozzi et al. 1995, Kouveliotou et al. 1995, Pendleton et al. 1996). However, caution is required in such studies, when dealing with the raw data. The effects of selection biases must be evaluated before obtaining these distributions and correlations. The parent distributions of the spectral parameters could be quite different from the observed distributions shown in the above figures. The differences are caused by the truncations resulting from the triggering procedure, and are a measure of trigger efficiencies for each of the four spectral parameters  $\alpha, \beta, E_p$ , and  $A$  or  $F_{tot} = A\xi(\alpha, \beta)$ . The truncation on  $A$  or  $F_{tot}$  is described by equation (1):  $F_{tot,lim} = F_{tot}(C_{min}/C_{max})$ . As mentioned previously and shown in detail in the next section, there are also selection biases against high and low values of  $E_p$ . For instance, BATSE is most likely to see bursts with  $E_p$  in the energy range in which the detector triggers. Because the detector needs some minimum number of counts  $C_{lim}$  to trigger, then for each burst one can find an interval  $[E_{pmin}, E_{pmax}]$  to which  $E_p$  is confined in order for the burst to have been detected.

Similarly, truncation is present for  $\alpha$  and  $\beta$ . For example, if a burst with given  $E_p$  and  $A$  had a value of  $\alpha$  which was positive and large or had a value of  $\beta$  which was negative and large, - i.e. if the  $\nu F_\nu$  spectrum had a steep rise or fall - then the observed  $C_{max}$  could fall below the threshold  $C_{min}$  and render the burst undetectable. Using the methods described in §2 and below, we can correct the raw distribution of all four parameters and determine their correlations with other GRB characteristics. However, the effect of the truncation on  $\alpha$  and  $\beta$  is more complicated and not as pronounced as that of  $E_p$  and  $F_{tot}$ . We will deal with the former in future publications. Here, we limit our discussion to obtaining the true distributions of  $E_p$  and  $F_{tot}$ . We will present the results from the Band spectrum fits to the burst only; the spectrum in equation (6) gives qualitatively similar results for all of the following analysis.

#### 4. Distribution of $E_p$

For each burst we have the values of  $\alpha, \beta, A, E_p$ , and the observed fluence  $F_{obs} = \int_{E_1}^{E_2} F_{\alpha,\beta,A}(E, E_p) dE$ , with  $E_1 = 50keV$  and  $E_2 = 300keV$ . From equation 1, we can calculate the fluence threshold  $F_{lim}$ . Using this limit, we can determine the possible range of values  $E_p$  can take on, and still trigger the BATSE instrument. It is clear that the limiting value  $E_{p,lim}$  must satisfy the equation

$$F_{lim} = \int_{E_1}^{E_2} F_{\alpha,\beta,A}(E, E_{p,lim}) dE. \quad (7)$$

For the spectral forms and parameter ranges discussed in the previous section, the right hand side of equation (7) increases monotonically with  $E_{p,lim}$ , reaches a maximum for  $E_{p,lim}$  within the limits of the integration, and then decreases monotonically. Consequently, there will be two values of  $E_{p,lim}$  that satisfy this equation. To find these two solutions, we start with the value of  $E_p$  determined by the simplex routine (for which the right side is equal to  $F_{obs}$ ), and increase it (while keeping  $\alpha$ ,  $\beta$ , and  $A$  equal to their determined values) until equation (7) is satisfied - that is, until the observed fluence is brought below the threshold. This value is the upper limit to  $E_p$ ,  $E_{p,max}$ . We then decrease  $E_p$  until this equation is again satisfied. This gives the lower limit  $E_{p,min}$ . In essence, the procedure amounts to redshifting/blueshifting the burst until it is undetectable by BATSE. Figure 2 shows  $E_p$  vs.  $E_{p,max}$  and  $E_{p,min}$  for the Band spectrum. Notice the truncation is much more prominent on the upper than the lower end; hence, we expect to see a more significant correction to the high end of the  $E_p$  distribution.

Using the method described in §2.3 for doubly truncated data, we corrected the observed distribution given that the observations can detect only bursts with  $E_p$  limited to the interval  $[E_{p,min}, E_{p,max}]$ . Figure 3 shows the raw and corrected differential distribution of  $E_p$  for the Band spectrum. The raw and corrected distributions are normalized such that they are equal at low values of  $E_p$  (where the data truncation is inconsequential). This normalization visually emphasizes the differences of the distributions at high  $E_p$ . The figures suggest that a large number of high  $E_p$  bursts are missed by the triggering procedure. These results are in qualitative agreement with Harris and Share (1997). Note that the statistical method we use to correct the  $E_p$  distribution places all of the probability on the observed distribution. This means that there will not be a correction to parts of the distribution in which there is no  $E_p$  observed by BATSE. Therefore, because we have no  $E_p$ 's below  $\sim 20$  keV, we cannot confirm Strohmeyer et al. (1998) reporting a significant number of low  $E_p$  bursts ( $< 20$  keV) observed by GINGA, but not observed by BATSE.

In order to determine the validity and significance of the difference between the distributions, we carry out the following two checks: First, we perform a K-S test on the cumulative distributions of  $E_p$ , and a  $\chi^2$  test on their differential distributions for both the Band spectrum and the smooth double power law. For the  $\chi^2$  test, we divide the distributions into two bins, with equal numbers of observed bursts per bin. As shown in the table below, in both cases, the tests indicate the probability that the observed and corrected  $E_p$  distributions are the same is extremely small.

Test	Spectrum	Probability the distributions same
K-S	Band	$1.8 \times 10^{-6}$
$\chi^2$	Band	$3.0 \times 10^{-7}$
K-S	Double Power Law	$4.4 \times 10^{-5}$
$\chi^2$	Double Power Law	$2.4 \times 10^{-5}$

Second, we have carried out simulations to determine the accuracy of the method described in



§2.3; Appendix A contains these results. We begin with a parent distribution of  $E_p$ 's, simulate an observational truncation (defined by the limiting fluence of the burst; see §4). From this we obtain our observed distribution of  $E_p$ 's. We then apply the above technique to correct for the truncation, and retrieve our parent distribution to very high accuracy, demonstrating the robustness of the method (see Appendix A for more details).

A bias against detection of high  $E_p$  bursts has significant implications on correlations of  $E_p$  with other measures of burst strength like peak flux,  $F_{obs}$ , or  $F_{tot}$ . The detector is most likely to miss the high  $E_p$  bursts with low strength, so that a simple correlation analysis between raw values of  $E_p$  and burst strength without the consideration of the data truncation can lead to erroneous correlations. Examples of studies which may be affected by such a bias include the correlation studies of Nemiroff et al. (1994) and Mallozzi et al. (1995). This will also have an important effect on determining whether or not the correlations are intrinsic or due to cosmological redshift (Brainerd, 1997). The above results indicate that a more thorough analysis of the correlations is required before conclusions can be reached on the redshifts or intrinsic effects. We will address this question in a future publication, when we have more accurate estimates of the spectral parameters.

## 5. Distribution of Ftot

As discussed in the introduction, an important way to learn about the spatial distribution of GRBs is to study the distribution of some standard candle variable of the event. We also conjecture the total radiated energy  $E_o$  may be the best candidate for such a standard candle variable, and that the total fluence  $F_{tot}$  of the GRB may provide the best measure of distance. Consequently, we study the distribution of the bursts' total fluence; if the burst radiates isotropically, the total fluence is related to the total emitted energy  $E_o$  as:

$$F_{tot} = \frac{E_o}{4\pi d_L^2}(1+z), \quad (8)$$

where  $d_L$ , the luminosity distance, depends on redshift and the cosmological model (Weinberg, 1972).

Again, because the detector is sensitive only over a finite energy range, BATSE does not necessarily obtain all photons from the burst. Hence, the detector measures only a portion of the burst's total fluence. However, the total fluence of a GRB can be obtained from the spectral fits to the observed fluence simply by integrating over the spectrum of that burst:  $F_{tot} = \int_{E_{min}}^{\infty} F_{\alpha,\beta,A}(E, E_p)dE$ . This fluence will have an observational lower limit in the same way that the fluence from 50 – 300 keV has, and its threshold is given by the generalization of equation (1):  $F_{tot,lim} \approx \frac{C_{min}}{C_{max}}F_{tot}$ . Following the steps described in Petrosian and Lee (1996), we first test for any correlation between  $F_{tot}$  and  $F_{tot,lim}$  and parametrically remove this correlation. We then use the method described in Efron and Petrosian (1994) for one sided truncated data (this is

equivalent to the method of §2.2, taking the upper limit  $u$  to  $\infty$ ), and obtain the cumulative and differential distributions for the total fluence.

Figures 4a and 4b show the cumulative and differential distributions of the total and observed fluence for our sample. Marked on each curve are GRB 970508 (circle) and GRB 971214 (cross). Following the tradition of radio astronomers (see Lee and Petrosian, 1996), we divide out the  $-3/2$  power law dependence of the number on the total fluence. In this way, deviation from the horizontal line suggests deviation from a homogeneous, isotropic, static, Euclidean distribution. In these figures, we have included all 518 bursts available - including those whose spectral fits gave high values of  $\chi^2$  - so as not to underestimate any part of these distributions. We have also applied the same procedure to the subsample of bursts with acceptable values of  $\chi^2$  and find that the distributions are similar to those of the complete sample within about 30 %.

Naturally, the total fluence of each burst will be larger than its observed fluence; however, the total and observed fluence distributions are qualitatively alike. The similarity of the distributions suggests that the spectral bias depicted in §4 has little influence on the distribution of the fluence. Note that the fluence distributions in Figure 4(a) and 4(b) are unlike the counts of other well known extragalactic sources such as galaxies, radio sources and AGNs or quasars. The transition from  $3/2$  power law is too abrupt and the slope beyond this transition is nearly constant. Clearly, some extraordinary evolutionary processes are at work. We explore this in more detail in the next section.

### 5.1. Rate Evolution

There have been several detailed analyses of the  $\log N$ - $\log S$  distribution for the peak fluxes of GRBs with inconclusive results. This is primarily because any observed distribution can be fitted to an arbitrary luminosity function and evolution even if one assumes a cosmological model (see e.g. Rutledge et al. 1995, Reichert and Mészáros, 1997, Mészáros and Mészáros, 1995, Hakkila et al., 1996). Additional uncertainty associated with these results comes from neglect of the time bias, spectral bias, and uncertainty in the value of the K-correction. These source of error are absent when dealing with the total fluence, which requires no correction for time bias (Lee and Petrosian, 1996), includes the spectral bias (described above), and requires no K-correction. Thus, the relation between the total fluence counts and either the cosmological models or the luminosity function and its evolution is more straight forward. Here we concentrate on the rate evolution of GRBs.

To obtain some indication of possible evolution, we assume several representative values for the total radiated energy  $E_o$  and derive the comoving rate density from the observed differential counts of the fluences as

$$\rho(z) = (1+z)n(F_{tot})(dV/dz)^{-1}(dF_{tot}/dz) \quad (9)$$

where  $n(F_{tot})$  is the differential distribution of the total fluence. Note that in all of our calculations, we have assumed  $H_o = 60\text{km s}^{-1}\text{Mpc}^{-1}$

Figures 5a, 5b and 5c show  $\rho(z)$  for three representative cosmological models. In order to span the range of possible evolutions, we choose three extreme cosmological models: a flat matter dominated model ( $\Omega_m = 1, \Omega_\Lambda = 0$ ), a curvature dominated model ( $\Omega_m = 0.2, \Omega_\Lambda = 0$ ), and a flat vacuum energy dominated model ( $\Omega_m = 0, \Omega_\Lambda = 1$ ). Here,  $\Omega_m$  is the density parameter (equal to the ratio of matter density to the critical density), and  $\Omega_\Lambda = \Lambda c^2/3H_o^2$  (where  $\Lambda$  is the cosmological constant). Within each figure,  $\rho(z)$  is plotted for four standard candle energies:  $E_o = 10^{51}, 10^{52}, 10^{53}, 10^{54}$  ergs. Superposed on each figure also is the star formation rate (SFR) from Madau et. al (1997, dotted line), this rate delayed by  $2 \times 10^9$  years (dashed-dot line), as well as the SFR convolved with a distribution of time delays  $P(t) \propto t^{-1}$  (solid curve), which may arise in a neutron star or black hole merger scenario (see e.g. Totani, 1997). Note that the SFR was calculated using an  $\Omega_m = 1, \Omega_\Lambda = 0$  cosmology (Madau, 1997); however, the shape of this curve as well as the 2 other curves derived from the SFR are fairly insensitive to the cosmological model (see e.g., Totani, 1997).

The dashed vertical line marks the observed redshift  $z = 0.83$  of GRB 970508 (Metzger et al., 1997); the dot-dashed vertical line marks the redshift  $z = 3.43$  of GRB 971214 (Kulkarni et al., 1998). The circle and the cross on each  $\rho(z)$  curve mark the theoretical redshifts of GRB 970508 and 971214 respectively, given the assumed value of  $E_o$  and their total fluences (calculated using the methods described in §3 and §5). Table II lists the required energy  $E_o$  - assuming isotropic emission - of GRB 970508 and GRB 971214 given their observational redshifts, their total fluences, and a cosmological model.

Burst	Redshift	$F_{tot}$	Cosmology	Required $E_o$
GRB 970508	0.83	$7.0 \times 10^{-6}$	$\Omega_m = 1 \Omega_\Lambda = 0$	$1.0 \times 10^{52}$
GRB 970508	0.83	$7.0 \times 10^{-6}$	$\Omega_m = 0.2 \Omega_\Lambda = 0$	$1.4 \times 10^{52}$
GRB 970508	0.83	$7.0 \times 10^{-6}$	$\Omega_m = 0 \Omega_\Lambda = 1$	$2.5 \times 10^{52}$
GRB 971214	3.43	$1.2 \times 10^{-5}$	$\Omega_m = 1 \Omega_\Lambda = 0$	$1.7 \times 10^{53}$
GRB 971214	3.43	$1.2 \times 10^{-5}$	$\Omega_m = 0.2 \Omega_\Lambda = 0$	$4.4 \times 10^{53}$
GRB 971214	3.43	$1.2 \times 10^{-5}$	$\Omega_m = 0 \Omega_\Lambda = 1$	$1.8 \times 10^{54}$

In all cases, the curve corresponding to  $E_o = 10^{51}$  ergs is ruled out by the observational data. The  $E_o \geq 10^{52}$  ergs curve accomodates GRB 970508, while GRB 971214 requires  $E_o > 10^{53}$  ergs. In the  $\Omega_\Lambda = 1$  case, the required  $E_o > 10^{54}$  ergs for GRB 981214 begins to exceed theoretical limits, which may be evidence against this cosmological model or evidence for strong beaming of the burst radiation. Our results suggest that the total gamma ray radiated energy is not a standard candle and is spread over at least one decade. We emphasize that these results depend critically on the total fluence, which in turn depends on accurate values for the spectral parameters for these bursts. Higher resolution fits to the data as well as more measurements of the redshifts

of bursts will allow us to constrain the curves more definitely.

Finally, note that none of the three curves for  $\rho(z)$  follow the star formation rate curve, as one would expect in many GRB models such as the merger or hypernovae models. The density evolution for GRBS is unlike that for AGN's or ordinary galaxies as well. The results agree - at least qualitatively - with those of Totani (1998). However, this is in contradiction with recent that the GRB rate follows the star formation rate (Wijers et al., 1998).

## 6. Summary and Conclusion

The primary aim of this paper has been to investigate the cosmological evolution of GRBs, which involves understanding the distributions of the spectral parameters as well as the total fluence of the burst. Selection effects limit the information we can observe to explore these distributions.

We have presented new non-parametric methods to account for these effects. We have applied these methods first to the distribution of the peak of the  $\nu F_\nu$  spectrum,  $E_p$ . We find that this spectral characteristic suffers both upper and lower thresholds, although the upper threshold has the dominant effect. We correct the observed distribution for this truncation and present the parent distribution of  $E_p$ . This contains a large number of high  $E_p$  bursts not evident in the observed distribution; this is important for studying correlations between  $E_p$  and other burst characteristics, as well as for theoretical considerations concerning GRB models.

Using the spectral fits for each burst, we determine a rough measure of the total gamma-ray fluence and present the GRB source counts based on this measure. We obtain both the differential and cumulative counts of the total and observed fluences.

We convert these distributions to the comoving rate density of GRBs for 3 different cosmological models and 3 different values of the total gamma ray radiated energies. We find that none of the curves follow the star formation rate as predicted by various GRB models. More observations on the redshifts of GRBs as well as high resolution spectral data (to obtain a precise value for the total fluence) are needed to substantiate these results.

As a final note, we summarize some of the caveats in our analysis. First, the spectral parameters are determined based on four channel data and are only rough estimates of the true spectral properties of the burst. In particular, because  $\beta$  is chosen from an assumed distribution, the correction to the  $E_p$  distribution could be overemphasized. These spectral parameters also affect the values of the total fluence (since  $F_{tot} = \int F_{\alpha,\beta,A}(E, E_p)dE$ ), which in turn affects the density evolution functions for the bursts. Furthermore, to derive the density curves, we have assumed that the bursts total fluence is a standard candle; although this seems to be the most plausible candidate for a standard candle, the observations of GRB 970508 and 971214 indicate the contrary. Note, however, that we can use a standard candle upper and lower limit to at least

constrain the possible evolution of GRBs. Finally, effects such as beaming were not taken into account in the density evolution analysis; this will affect the amount of energy we assume for the burst as well as the number of burst occurrences over some time interval. The observed dispersion in the total radiated energy (about an order of magnitude or higher) could be due to variation in the degree of beaming.

We would like to acknowledge P. Madau for the star formation rate data used to generate the three SFR curves in Figures 5 (a),(b), and (c). We would also like to thank B. Efron for help in implementing the statistical methods discussed in the text. Finally, N.M. Lloyd would like to thank members of the BATSE team for many useful discussions, and their hospitality during her visit to MSFC.

## A. Appendix

Here, we describe the results of simulations which exhibit the technique and demonstrate the accuracy of the procedure used for correcting doubly truncated data. For this analysis, we use the Band spectrum displayed in equation 5. We pull  $E_p$  from a uniform distribution between 5 and 35 keV.  $\alpha$  is also drawn from a uniform distribution ranging between -0.9 and 5.9, as was  $\beta$  which ranged from -9.0 to -2.1. Finally, our normalization parameter  $A$  is taken from a uniform distribution from  $12 \times 10^{-9}$  to  $18 \times 10^{-9}$  ergs/cm<sup>2</sup>. Note that we are not trying to simulate the real distribution of any of these parameters - we choose these distributions for the purpose of displaying selection effects and to what degree our method can account for them.

Once we have the spectral parameters, we can calculate the fluence in each of the four BATSE LAD energy channels. The limiting fluence of each burst is chosen from a gaussian distribution with a mean of  $6 \times 10^{-11}$  ergs/cm<sup>2</sup> and a standard deviation of  $6 \times 10^{-10}$  ergs/cm<sup>2</sup> (note again, this is not an attempt to simulate the actual BATSE detector response). We then ask the question: How many of the 1000 simulated bursts have their fluence in channels 2 and 3, greater than the limiting fluence? We find 554 bursts survived this cut - we will call this the observed sample. We then proceed to apply the method described in §2 to our observed sample, to see if we could get back the original distribution of  $E_p$ 's. Figure 6 shows the the parent sample, the observed sample, and the correction to the observed sample. As evident, the correction accounts for the truncated data, and approximately reproduces the original sample. See §2 for a full description of the technique.

## REFERENCES

- Band, D., et al. 1993, *ApJ*, 413, 281
- Brainerd, J.J. 1997, *ApJ*, 487, 96
- Efron, B. & Petrosian, V. 1992, *ApJ.*, 399, 345
- Efron, B. & Petrosian, V., *JASA*, in press
- Galama, T., et al. 1997, in *Gamma Ray Bursts*, AIP Conf. Proc. 428, eds. C.A. Meegan, R.D. Preece, T.M. Koshut (New York: AIP) , 478
- Hakkila, J., et al. 1996, in *Gamma Ray Bursts*, AIP Conf. Proc. 307, eds. G.J. Fishman, J.J. Brainerd, K.Hurley (New York: AIP), 387
- Harris, M.J. & Share, G.H. 1997, in *Gamma Ray Bursts*, AIP Conf. Proc. 428, eds. C.A. Meegan, R.D. Preece, T.M. Koshut (New York: AIP) , 314
- Horack, J.M., Emslie, A.G., Hartmann, D.H. 1995, *ApJ*, 447, 474
- Kouveliotou, C., et al. 1995, in *Gamma Ray Bursts*, AIP Conf. Proc. 384, eds. C Kouveliotou, M.S. Briggs, G.J. Fishman (New York: AIP), p.42
- Kulkarni, S., et al. 1998, *Nature* 393, 35
- Lee, T. & Petrosian, V. 1996, *ApJ*, 470, 479
- Lloyd, N.M & Petrosian, V. 1997, in *Gamma Ray Bursts*, AIP Conf. Proc. 428, eds. C.A. Meegan, R.D. Preece, T.M. Koshut (New York: AIP) , 67
- Madau, P. 1997, *astro-ph/9709147*
- Mallozzi, R.S., et al. 1995, *ApJ*, 454, 597
- Maloney, A. & Petrosian, V. 1998, *ApJ*, in press
- Meegan, C., et al. 1992, *Nature*, 355, 143
- Meegan, C., et al. 1995, *ApJS*, 106, 65
- Mészáros, P. & Mészáros, A. 1995, *ApJ*, 449, 9
- Metzger et al. 1997, *Nature*, 387, 879
- Murakami, T. et al. 1997, in *Gamma Ray Bursts*, AIP Conf. Proc. 428, eds. C.A. Meegan, R.D. Preece, T.M. Koshut (New York: AIP) , 435
- Nemiroff, R.J., et al. 1997, *ApJ*, 435, L113

- Pendleton, G.N., et al. 1996, ApJ, 464, 606
- Petrosian, V. 1992, in Statistical Challenges in Modern Astronomy, eds. E.D.Feigelson and G.J. Babu (New York: Springer-Verlag), 173.
- Petrosian, V. 1993, ApJ, 402, L33
- Petrosian, V. & Lee, T. 1996, ApJ, 467, L29
- Piran, T. & Narayan, R. 1995, in Gamma Ray Bursts, AIP Conf. Proc. 384, eds. C Kouveliotou, M.S. Briggs, G.J. Fishman (New York: AIP), 233
- Press, W. H., Teukolsky, S. A., Vetterling W. T., and Flannery, B. P. 1992, Numerical Recipes in FORTRAN (Cambridge: Cambridge University Press)
- Reichert, D.E. & Mészáros, P. 1997, ApJ, 483, 597
- Rutledge, R.E., et al. 1995, MNRAS, 276, 753
- Strohmeyer, T.E., et al. 1997, astro-ph/9712332
- Totani, T. 1997, ApJ, 486, L71
- Totani, T. 1998, astro-ph/9805263
- Weinberg, S. 1972, Gravitation and Cosmology: Principles and Applications of the General Theory of Relativity (New York: Wiley)
- Wijers, R.A.M., et al. 1998, MNRAS, 294, L13

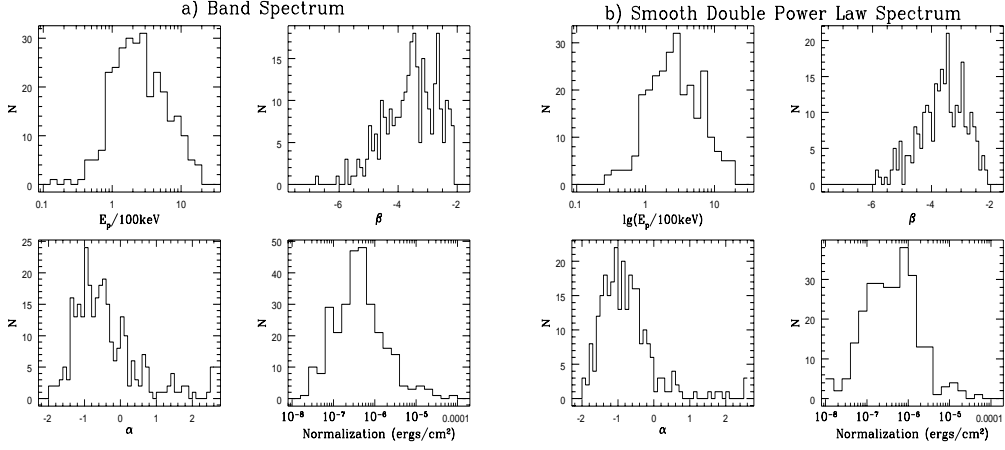


Fig. 1.— The distribution of the spectral parameters determined from a) the Band spectrum and b) a smooth double power-law spectrum respectively. Note that  $\beta$  is drawn from the same truncated gaussian distribution in both cases, and is not a fitted parameter.

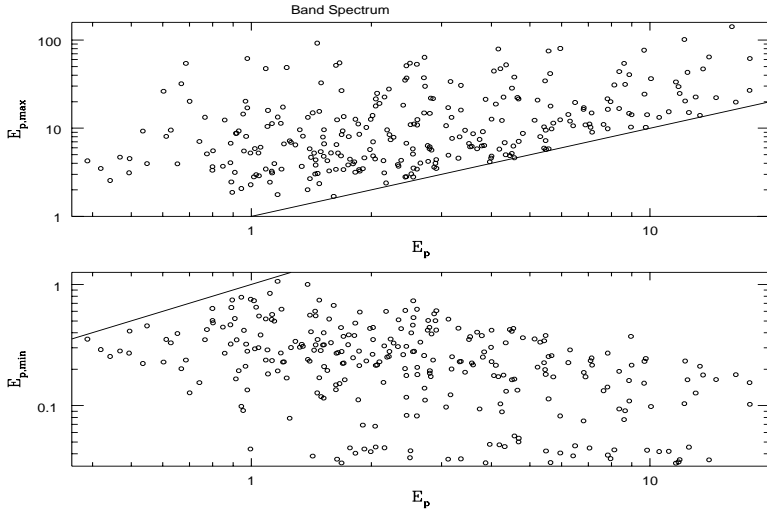


Fig. 2.— The maximum and minimum values of  $E_p$  for the Band spectrum. Note that the truncation is more severe from above than below, which indicates that observations may miss a population of GRBs with high  $E_p$ .



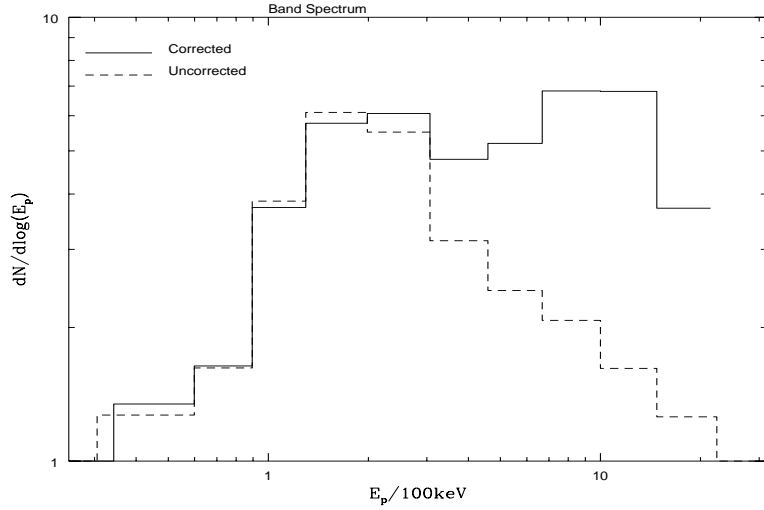


Fig. 3.— The observed and “corrected” distribution of  $E_p$  for the Band spectrum. The figure suggests that there is a significant population of high  $E_p$  bursts undetected by BATSE. As mentioned in the text, the methods we used will not produce a correction beyond the raw observed distribution.

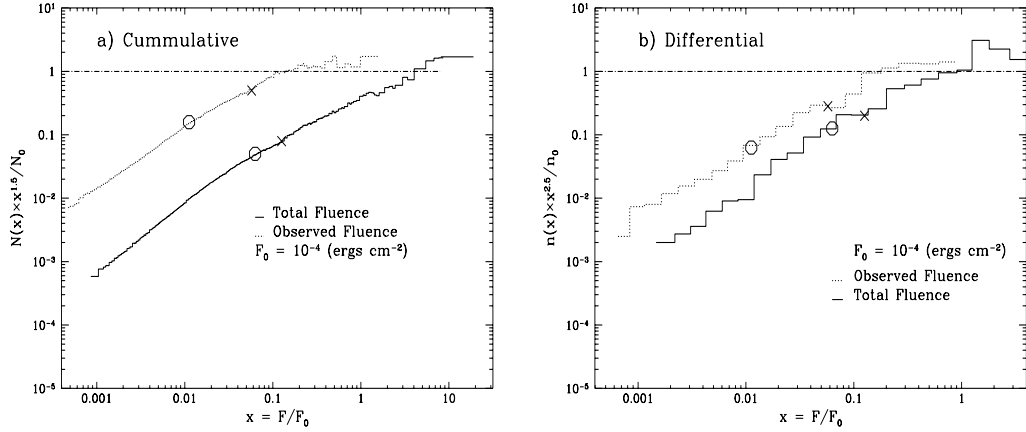


Fig. 4.— The cumulative (a) and differential (b) distributions of both the observed ( $F_{obs}$ ) and total ( $F_{tot}$ ) fluences. The circles indicates the observed and total fluences of GRB 970508, and the cross marks the observed and total fluences of GRB 971214. In each figure, note the similarities between the two distributions; they both display an abrupt break from the HISE dependence (see text), indicating presence of strong evolutionary processes.

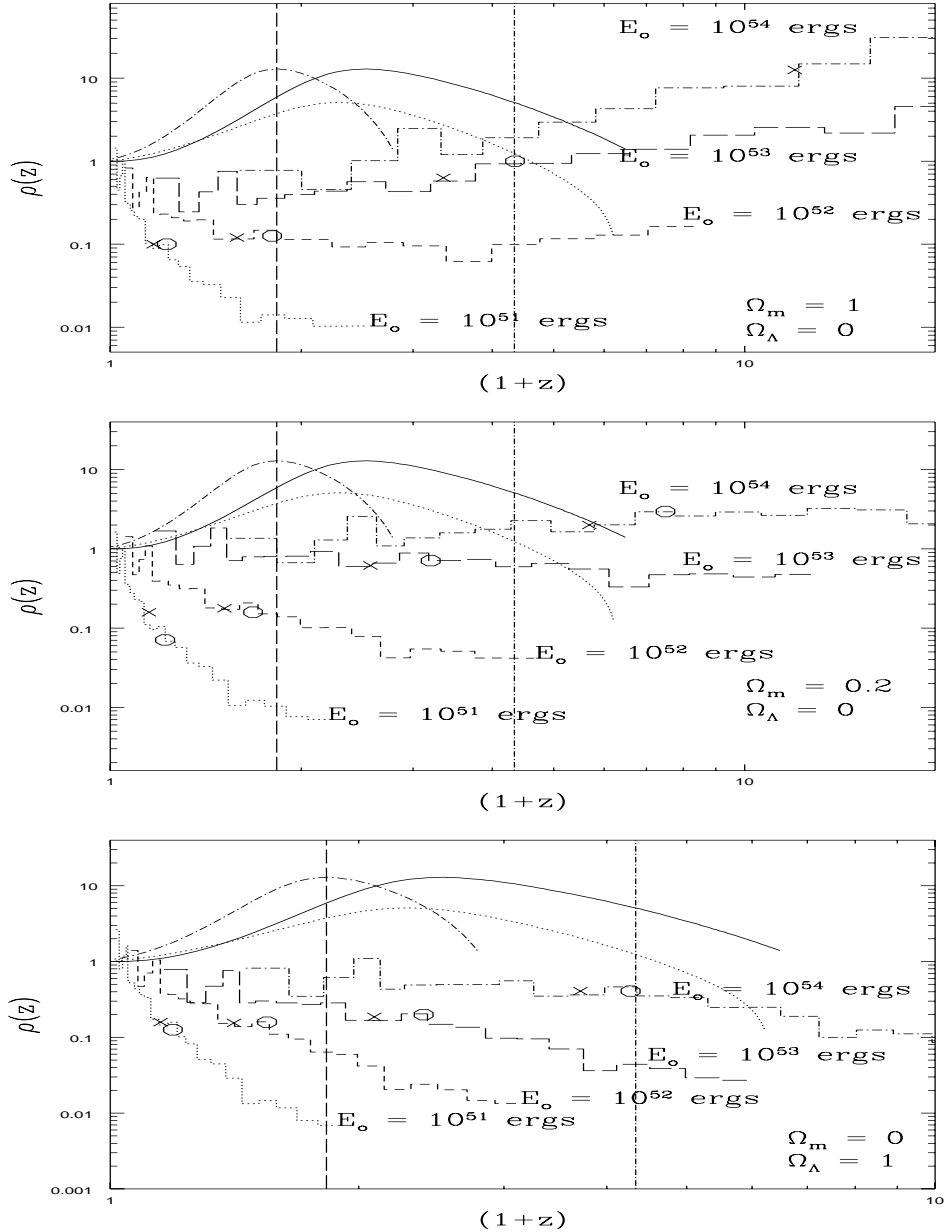


Fig. 5.— The comoving rate density versus redshift  $z$  for 3 different cosmological models indicated by the values of  $\Omega_m$  and  $\Omega_\Lambda$ . Within each plot, we show the rate density for 4 different standard candle energies. Note that these curves are significantly different from: 1) the star formation rate (SFR) from Madau et al., 1997 (solid line), 2) the star formation rate with a time delay of  $2 \times 10^9$  yr (dot-dash line), and 3) the star formation rate convolved with a distribution of time delays (dotted line, Totani et al., 1997). The observed redshifts of bursts 970508 and 971214 are indicated by the dashed vertical lines. The circles and crosses mark the theoretical redshift of burst 970508 and 971214, given the respective standard candle energy and their total fluences. Note that no single standard candle energy can accommodate the observed redshifts of these bursts, in any of the three models.

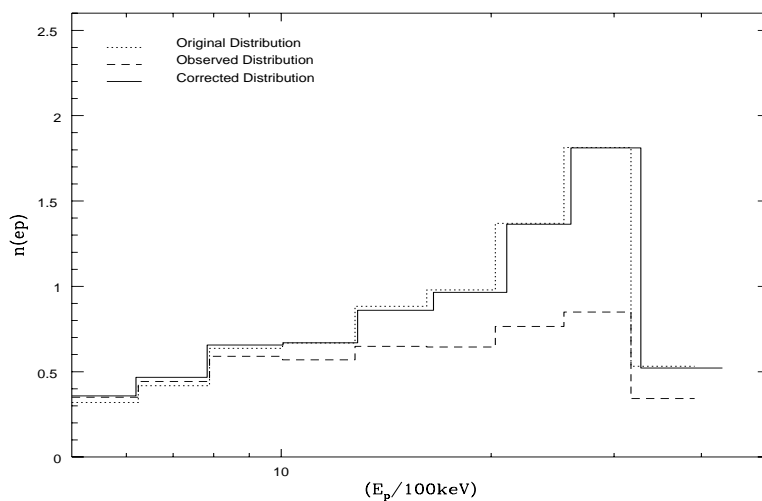


Fig. 6.— The original  $E_p$  distribution (solid line), the observed  $E_p$  distribution given the criterion  $F_{obs} > F_{lim}$  (dashed line), and the corrected distribution using the method described in §2 of the text (dotted line). These distributions are obtained from the simulations described in the Appendix. Note that the procedure recovers the original distribution almost exactly. Any differences are primarily due to differences in the binnings of the distributions.